A Combined Proteome and Microarray Investigation of Inorganic Phosphate-induced Pre-osteoblast Cells*⒮

Kelly A. Conrads‡§, Ming Yi§¶, Kerri A. Simpson‡§, David A. Lucas‖, Corinne E. Camalier‡, Li-Rong Yu‖, Timothy D. Veenstra‖, Robert M. Stephens¶, Thomas P. Conrads‖, and George R. Beck, Jr.‡**

Inorganic phosphate, which is generated during osteoblast differentiation and mineralization, has recently been identified as an important signaling molecule capable of altering signal transduction pathways and gene expression. A large scale quantitative proteomic investigation of pre-osteoblasts stimulated with inorganic phosphate for 24 h resulted in the identification of 2501 proteins, of which 410 (16%) had an altered abundance ratio of greater than or equal to 1.75-fold, either up or down, revealing both novel and previously defined osteoblast-regulated proteins. A pathway/function analysis of these proteins revealed an increase in cell cycle and proliferation that was subsequently verified by conventional biochemical means. To further analyze the mechanisms by which inorganic phosphate regulates cellular protein levels, we undertook a mRNA microarray analysis of pre-osteoblast cells at 18, 21, and 24 h after inorganic phosphate exposure. Comparison of the mRNA microarray data with the 24-hour quantitative proteomic data resulted in a generally weak overall correlation; the 21-hour RNA sample showed the highest correlation to the proteomic data. However, an analysis of osteoblast relevant proteins revealed a much higher correlation at all time points. A comparison of the microarray and proteomic datasets allowed for the identification of a number of candidate proteins that are post-transcriptionally regulated by elevated inorganic phosphate, including Fra-1, a member of the activator protein-1 family of transcription factors. The analysis of the data presented here not only sheds new light on the important roles of inorganic phosphate in osteoblast function but also begins to address the contribution of post-transcriptional and post-translational regulation to a cell's expressed proteome. The ability to accurately measure changes in both protein abundance and mRNA levels on a system-wide scale represents a novel means to extract data from previously one-dimensional datasets. *Molecular & Cellular Proteomics 4:1284–1296, 2005.*

Numerous factors determine both the initial cellular response and ultimate cellular adaptation to a given stimulus or insult. The terminal phenotype of a given cell response remains a poorly understood combination of changes in signal transduction pathways, promoter regulation, mRNA processing and subsequent protein abundance, and post-translational regulation of proteins. The challenge of large scale gene expression profiling has been met, leaving the goal of fully understanding the cellular response to a given stimulus or changing environment limited by the inability to fully evaluate the proteome. The ability to conduct an analysis of changes in both protein abundance and RNA levels on a "systems level" scale sufficient to entirely enumerate the response of a cell will undoubtedly be a powerful tool in assessing not only complex cellular processes, such as differentiation, but should also provide clues as to how to manipulate the cell phenotype by intervention.

The process of osteoblast differentiation leading to bone mineralization is a poorly understood series of temporally and spatially coordinated events occurring on the order of weeks and months. A significant end point in this process is the creation of a mineralized matrix that consists mainly of collagen, non-collagenous proteins and hydroxyapatite $(Ca_{10}(PO_4)_6(OH)_2)$. During this process, osteoblasts are exposed to high levels of inorganic phosphate. Using the MC3T3-E1 osteoblast differentiation model (1–3), we have recently described the significance of inorganic phosphate, which is generated during differentiation, as a signaling molecule capable of altering specific signal transduction pathways, gene expression, and ultimately mineralization (4, 5). Furthermore, a number of studies have demonstrated the ability of inorganic phosphate to alter gene expression and or cell function in other cell types, including parathyroid (6), neurons (7), kidney (8), vascular smooth muscle (9), chondrocytes (10), and osteoclasts (11). Hence, a more complete understanding of the consequences of elevated inorganic phosphate on cell function may be relevant not only to the

process of osteoblast differentiation but also to various cell types with a wide range of functions. Toward this end, we were interested in determining how inorganic phosphate affects protein abundance levels and how these effects correlate with changes in gene expression at transcriptional levels in the MC3T3-E1 osteoblast differentiation model.

The aims of this study were to determine the affect of elevated phosphate on the osteoblast proteome and to evaluate this effect at a systems level by comparing microarray and proteomic datasets. Herein, we report the identity and comparison of changes of relative abundance of more than 2,500 proteins measured in control and inorganic phosphate-treated MC3T3-E1 pre-osteoblast cells using cleavable isotope-coded affinity tag reagents and mass spectrometry. The methods used to derive this dataset have been described previously (12). Four hundred and ten proteins (corresponding to ~16% of all proteins identified) showed a change in relative abundance of $\geq$1.75-fold, either up or down, when the cells were treated with inorganic phosphate. This large number of differentially abundant proteins underscores the significance of inorganic phosphate as a signaling molecule. A comparison of the proteomic dataset with multiple mRNA microarray analysis at time points preceding the cICAT data revealed an overall low correlation, although specific subgroups of proteins/genes based on functional categorization or pathway analysis demonstrated much higher correlations. The comparison of genomic and proteomic datasets led to the identification of Fra-1, an important bone regulatory transcription factor, as an inorganic phosphate regulated protein. The datasets reported here not only shed light on the effects of inorganic phosphate on osteoblast function but also reveal novel systems level relationships as to the nature of transcription and translation.

EXPERIMENTAL PROCEDURES

Materials—Dibasic sodium phosphate (Na_2HPO_4), monobasic sodium phosphate (NaH_2PO_4), cycloheximide, and actinomycin D were purchased from Sigma. Sodium sulfate (Na_2SO_4) was from Valeant Pharmaceuticals (Costa Mesa, CA). Propidium iodide was purchased from Roche Diagnostics Corp. Radiochemicals were obtained from PerkinElmer Life Sciences. 12-*O*-tetradecanoylphorbol-13-acetate (TPA)[1] was kindly provided by Nancy Colburn (National Cancer Institute, Frederick, MD).

Immunoblotting—MC3T3-E1 osteoblast cells, cultured as described previously (12), were treated with 10 mM inorganic phosphate or inorganic sulfate (control) for 24 h and harvested in PBS. Total cell lysate was generated by lysis in p300 lysis buffer (20 mM sodium dihydrogen phosphate, 250 mM sodium chloride, 30 mM sodium pyrophosphate, 0.1% Nonidet P-40, 5 mM EDTA, and 10 mM sodium fluoride, adjusted to pH 7.0) supplemented with the following protease inhibitors at the indicated final concentrations: 2.0 μg/ml aprotinin, 2.0 μg/ml leupeptin, 1.0 μg/ml pepstatin, 100 μM sodium ortho

---

[1] The abbreviations used are: TPA, 12-*O*-tetradecacanoylphorbol-13-acetate; cICAT, cleavable ICAT; GO, gene ontology; AP-1, activator protein-1; Fra-1, fos-related antigen-1; ERK, extracellular signal-regulated kinase.

vanadate, and 1 mM dithiothreitol. For nuclear and cytoplasmic fractionation, MC3T3-E1 cells were treated as above and harvested in PBS. To obtain the cytoplasmic fraction, cells were lysed in 10 mM Tris HCl, 10 mM NaCl, 3 mM $MgCl_2$, and 0.5% Nonidet P-40 supplemented with protease inhibitors as described above. After centrifugation (2000 rpm for 10 min) and removal of the cytoplasmic fraction, the nuclear pellet was lysed in p300 lysis buffer as described above and centrifuged at 13,200 rpm for 10 min. The protein concentration of the cell lysates was determined with a BCA protein assay reagent kit (BioRad Laboratories). 50 μg of lysate was resolved on a NuPAGE 4–12% Bis-Tris gel (Invitrogen). After electrophoresis, proteins were transferred to Hybond-P membrane (Amersham Bisociences) according to the manufacturer's protocol. The membrane was blocked with 3% milk in Tris-buffered saline/Tween 20 (20 mM Tris, pH 7.5, and 150 mM NaCl) before addition of antibody, except osteopontin, which was blocked in 5% milk. The blots were visualized by chemiluminescence development using a Western blotting Detection System (Amersham Bisociences). Antibodies, Fra-1, histone deacetylase 1, proliferating cell nuclear antigen, protein kinase Cι, and actin were purchased from Santa Cruz Biotechnologies Inc. (Santa Cruz, CA), p21 and PKC alpha from Pharmingen (BD Biosciences, Franklin Lakes, NJ), ERK1/2 from (Promega, Madison, WI) and cyclin D1 antibody (Cell Signaling Technologies Inc., Beverly, MA).

Quantitation of Western Blot—Densitometric analysis of the Western blot was performed using the Kodak Digital Science 1D program. The region of interest was defined using a rectangular box with identical interior pixel area for both sulfate and phosphate-treated samples, although the pixel area varied for different proteins. The dimension of the box was fitted to the larger of either the sulfate or phosphate bands by hand. The net intensity as determined by the program was used to calculate -fold induction or repression = [phosphate (net)/sulfate (net)].

Function Analysis—Data were analyzed using Ingenuity pathway analysis application (www.ingenuity.com). Only the cICAT datasets representing proteins with changes in abundance of 1.75 or more were used (Supplemental Tables III and IV) for this analysis.

Proliferation Assay—MC3T3-E1 cells were plated in 96-well plates at a density of 2,500 cells per well. Seventy-two hours after plating, cells were treated with 10 mM inorganic phosphate or sulfate (control). After treatment for the indicated length of time, cell titer reagent (Promega's Celltiter 96 aqueous one solution cell proliferation assay) was added to each well following the manufacturer's protocol. After addition of reagent, plate was incubated at 37 °C and absorbance readings (490 nm) were taken at 2 h (BioRad Lumimark microplate reader).

Flow Cytometry—Seventy-two hours after plating, MC3T3-E1 cells were treated with 10 mM inorganic phosphate or sulfate for the indicated times. Cells were then rinsed with ice-cold PBS, scraped off the culture dishes, and pelleted by centrifugation at 2,000 rpm for 2 min. Cell pellets were resuspended in 0.3 ml of ice-cold PBS followed by addition of 0.7 ml of ice-cold 100% ethanol. Samples were washed twice with 1 ml of ice-cold of PBS and resuspended in 0.9 ml of PBS. RNase A (Invitrogen) was added to each sample and incubated for 15 min. Propidium iodide (20 μl of 0.5 mg/ml) was added to each sample 1 hour before analysis by flow cytometry (Laboratory of Experimental Immunology, NCI-Frederick).

Cleavable ICAT Labeling and Affinity Purification—The methods used in the derivation of this particular dataset are described in more detail in Ref. 12. In brief, MC3T3-E1 osteoblast cell proteins (~750 μg each) were labeled either with the light (control, cICAT-$^{13}C_0$) or the heavy (phosphate-treated, cICAT-$^{13}C_9$) isotopic versions of the cICAT reagent using a method modified from that recommended by the manufacturer. An UltraLink immobilized monomeric avidin column was slurry-packed in a glass Pasteur pipette and equilibrated. The

column was blocked, the biotin was stripped from the reversible binding sites of the column per the manufacturer's instructions, and the column was re-equilibrated. The cICAT-labeled peptides were boiled, cooled to room temperature, and loaded onto the avidin column and allowed to incubate for 15 min at ambient temperature. After the column was washed, the cICAT-labeled peptides were eluted and lyophilized to dryness. The biotin moiety was cleaved from the cICAT-labeled peptides by treatment with the cleaving reagents provided by the manufacturer and lyophilized to dryness.

Strong Cation Exchange Fractionation and Microcapillary Reversed-phase LC-MS/MS of cICAT Labeled Peptides—Again, these methods are described in more detail in Ref. 12. The lyophilized MC3T3-E1 osteoblast cICAT-labeled peptides were dissolved and injected onto a strong cation-exchange LC column (PolyLC Inc., Columbia, MD). A multistep gradient was used to elute the cICAT-labeled peptides from the column. Each strong cation-exchange LC fraction was lyophilized and reconstituted before microcapillary reversed-phase LC-MS/MS. 10-cm microcapillary reversed-phase LC ESI columns were coupled online with an ion-trap MS (LCQ Deca XP, ThermoElectron, San Jose, CA) to analyze the cICAT labeled peptides from the MC3T3-E1 osteoblast cells. After loading the sample, the cICAT-labeled peptides were eluted using a linear step gradient. The ion-trap MS was operated in a data-dependent tandem MS (MS/MS) mode in which each full MS scan was followed by three MS/MS scans, where the three most abundant peptide molecular ions were dynamically selected for CID using a normalized collision energy of 35%. The MS spectrum for the molecular ions was acquired using two microscans for the mass range of m/z 475–2000 and the CID spectrum for the fragment ions was acquired using three microscans. Dynamic exclusion was used to minimize redundant acquisition of peptides previously selected for MS/MS. The heated capillary temperature and electrospray voltage were set at 160 °C and 1.7 kV, respectively.

Peptide Identification and Quantitation—The raw MS/MS data acquired on the ion-trap MS were searched using SEQUEST against the *Mus musculus* proteome database (27,612 entries) downloaded from the European Bioinformatics Institute (EBI; www.ebi.ac.uk/proteome/index.html). The *Archaea*-derived database (12,038 entries) used in the false-positive bioinformatic analysis was constructed using genomic sequence information from the following organisms: *Aeropyrum pernix*, *Archaeoglobus fulgidus*, *Pyrobaculum aerophilum*, *Sulfolobus tokodaii*, and *Thermoplasma volcanium*. Dynamic modifications for cysteinyl (Cys) residues were set by mass additions of the cleaved cICAT labels (227.13 Da for the light label, 236.16 Da for the heavy label) in a single search. SEQUEST criteria were set as Xcorr $\geq$ 1.9 for $[M+H]^{1+}$ ions, $\geq$ 2.2 for $[M+H]^{2+}$ ions, and $\geq$ 2.9 for $[M+H]^{3+}$ ions, and DeltaCn $\geq$ 0.08 for the identification of fully tryptic peptides within the cICAT-labeled samples. The identified peptides were quantified using XPRESS (Thermo Electron, San Jose, CA), which calculates the relative abundances ($^{13}C_9/^{13}C_0$, in this dataset) of peptides based on the area of their extracted ion chromatograms.

RNA Isolation and Northern Blotting—Total cell RNA was prepared using TRIzol reagent (Invitrogen) according to manufacturer's recommendations. 10 μg of RNA was loaded per lane and separated by electrophoresis through a 1% formaldehyde-agarose gel. The RNA was transferred to a Hybond-N nylon membrane (Amersham Biosciences) and cross-linked by UV irradiation and baking at 80 °C. ^{32}P-labeled probes were prepared using a random prime labeling kit (Roche Applied Science). Between successive probes, blots were stripped by treatment with boiling 0.1% SDS.

Plasmids Used for Northern Probes—The Fra-1 plasmid was provided by Nancy Colburn (NCI-Frederick) and described in Ref. 13. The osteopontin plasmid, mop3, was provided by Marian Young and described in Ref. 14. The actin probe has been described previously (15).

Microarray—Oligo arrays (22,272), print Mm-FCRF-CGEN1ext-v4p4_082703, were printed by the Laboratory of Molecular Technology (Frederick, MD) and described at nciarray.nci.nih.gov/cgi-bin/gipo. Total RNA (10 μg) was labeled with either Cy3 or Cy5 Mono-Reactive Dye (Amersham Biosciences) using Superscript Indirect cDNA Labeling System (Invitrogen) following the manufacturer's protocol. Cy3- and Cy5-labeled RNA were combined in Tris-EDTA and concentrated using Microcon Y-30 spin columns (Millipore, Bedford, MA). Once recovered, 10 μg of mouse COT-1 DNA (Invitrogen), 8–10 μg of polyA (Amersham Biosciences), and 4 μg of yeast tRNA (Sigma) were added to the RNA along with freshly made F-hybridization buffer (50% formamide, 10× SSC, and 0.2% SDS), and the solution was transferred to 42 °C until ready for use. Arrays were prehybridized at 42 °C for 1 h (5× SSC, 0.1% SDS, 1% BSA) followed by washing in sterile H_2O and isopropanol and allowed to dry for not more than 1 h. Labeled probe was hybridized to the microarray overnight at 42 °C. Arrays were washed for 2 min in each of the following: 2× SSC, 0.1% SDS; 1× SSC, 0.1% SDS; and 0.2× SSC and then briefly in 0.05× SSC. Arrays were spun dry in a centrifuge at 50 × g for 10 min and scanned. Arrays were scanned using a GenePix microarray scanner (Axon Instruments, Union City, CA), and data were analyzed by GenePix Pro 4.0.

Correlation Coefficient Calculation and Validation—To correlate mRNA abundance to protein abundance for entire datasets, Pearson correlation coefficients were calculated using R-package (www.r-project.org) for each pair of the entire cICAT dataset and one of the microarray datasets (18, 21, and 24 h, and the microarray dataset using duplicate samples as used for cICAT "array").

To correlate mRNA abundance to protein abundance within individual pathways or Gene Ontology (GO) term scope, pathway-scope correlation coefficients were calculated for each pathway from the Biocarta collection (www.biocarta.com) or each GO term-associated group (Biological Processes, www.geneontology.org), which has at least three genes that have valid data in the dataset pairs for calculation. In brief, genes and their associated data from the whole datasets were sorted into subgroups based on whether they belonged to individual pathways or GO groups by using a pathway-based analysis software package developed in Advanced Biomedical Computing Center, NCI and SAIC-Frederick (initially supported by University of Texas Southwestern Medical Center at Dallas (http://wps.swmed.edu)). The software is also used to map and unify IDs of all the genes, including protein IDs and GenBank IDs from microarray or cICAT datasets. Then, the correlation coefficients for genes in each pathway or GO group that have at least three genes with valid data in between the dataset pair of cICAT and one of microarray datasets (18, 21, and 24 h and the microarray dataset using the same cells as used for cICAT) are calculated as a batch using R-package with the Pearson method (genes with missing values in one of the dataset pairs were not put into calculation for correlation coefficients). The results are parsed into a tabular format for representation purposes. The statistical significance of the results was validated using permutation analysis. In brief, the permutation analysis is done with a utility program for permutation of the data and R-package for statistical calculation of correlation coefficients for data in each of the permutated data files. To obtain permutated correlation coefficients for each candidate pathways or GO groups to be validated, each gene and its data in the pathway or GO group is shuffled randomly within the data pool of the corresponding dataset to generate a permutated file with the same number of genes as the original file but with permutated data. This process is iterated for 1000 times to generate 1000 permutated files for each intended pathway or GO group. Then correlation coefficients for each permutated data file were calculated using R-package with the Pearson method as described above.

TABLE I

Partial list of inorganic phosphate-responsive proteins

n, number of peptides identified; Avg., average change in abundance (phosphate/control).

Protein description	n	Avg.	S.D.	Accession no.
Increased abundance				
Extracellular matrix				
α-2-macroglobulin-P	4	51.25	38.81	Q811S0
AMBP protein (Bikunin)	1	20.00		Q07456
ADAMTS-2	1	10.00		Q8C9W3
Extracellular matrix protein 1	10	5.01	9.96	Q61508
Polycystin 2	1	5.00		O35245
Metallopr. Inhib.1 (TIMP-1)	5	3.15	0.81	P12032
α-2-HS-glycoprotein	7	1.75	1.10	P29699
Transcriptional regulators				
Zinc finger protein 30	1	10.00		Q60585
Steroid receptor coactivator-1	1	9.09		P70366
Fos-related antigen-1 (FRA-1)	2	3.15	1.44	P48755
Signaling				
Plectin	17	5.89	9.21	Q9QXS1
GXII sPLA2	2	4.66	3.51	Q9EPR2
MAPKK 3	4	3.35	2.54	O09110
Citron protein	1	3.13		P49025
Intracellular Regulators				
Butyrate resp. fctr 2 (TIS11D)	2	2.80	0.33	P23949
Ubi-conjugating enzyme E2	6	2.34	1.64	O88738
Copine I	9	2.14	3.41	Q8C166
Receptors/transporters				
Na^{2+}-dependent dopamine transport	1	11.11		Q61327
Thrombin receptor (PAR-1)	1	4.55		P30558
Mitochondrial (OXPHOS)				
Cytochrome b_5 reductase	4	8.54	11.15	Q9DCN2
NADH-ubiquinone oxi. B17.2	1	8.33		Q7TMF3
Ubiquinol-cytochrome c reductase	2	4.98	5.81	Q9DB77
NADH-ubiquinone oxi PDSW	4	4.36	6.62	Q9DCS9
Adenosine kinase	1	4.35		Q91VJ3
Cytochrome c_1	3	3.15	3.46	Q9D0M3
ADP,ATP carrier protein	8	2.80	2.70	P51881
Hexokinase type II	3	2.58	2.10	O08528
NAD(P) transhydrogenase	9	2.28	3.89	Q61941
Decreased abundance				
Extracellular matrix				
Decorin (PG-S2)	1	0.33		P28654
Tropomyosin 2 (β-chain)	2	0.33	0.00	P58774
Periostin	5	0.44	0.14	Q62009
Osteoglycin (Mimecan)	1	0.45		Q62000
Collagen α1(V)	5	0.48	0.50	O88207
Emilin 1	2	0.54	0.17	Q99K41
Chondroitin 4-O-sulfotransferase	2	0.56	0.45	Q9JJS3
Transcriptional regulators				
Nuc. receptor co-repressor 2	1	0.07		Q9WU42
α-globin tran. factor CP2	1	0.44		Q9ERA0
AT motif-binding factor	1	0.48		Q61329
Signaling				
Serine-protein kinase ATM	1	0.11		Q62388
Transforming protein RhoC	3	0.13	0.18	Q62159
BMP 3b (GDF-10)	1	0.15		P97737
Tyrosine-protein kinase JAK1	1	0.27		P52332

TABLE I—*continued*

Protein description	n	Avg.	S.D.	Accession no.
Intracellular Regulators				
JAZ (Zfp346)	1	0.16		Q9R0B7
ECSIT	1	0.38		Q9QZH6
SDF2L1	2	0.20	0.00	Q9ESP1
Receptors/transporters				
Fgfr2	1	0.15		P21803
DAAM 2	1	0.33		Q80U19
Mitochondrial (β-oxidation)				
Carnitine O-palmitoyltransferase	1	0.31		P52825
Putative D2,D4-dienoyl-CoA	1	0.40		Q99MZ7
Propionyl CoA carboxylase α	1	0.46		Q91ZA3
Acyl-CoA acetyltransferase	4	0.48	0.30	Q8QZT1
D2,D4-dienoyl-CoA reductase	2	0.56	0.03	Q9WV68
Acyl-CoA dehydrogenase	2	0.59	0.02	Q9DBL1

RESULTS

In this study, we report a functional characterization and correlation analysis of more than 2501 proteins in MC3T3-E1 pre-osteoblasts and the relative change in abundance in response to elevated inorganic phosphate identified by cICAT. The technique used to derive this dataset is described in more detail in Ref. 12. A complete summary of the proteins identified in this study with the average change in abundance is presented in Supplemental Table I, and a complete summary of all peptides identified is presented in Supplemental Table II. The generation of such a large dataset, ~9% of the proteins currently predicted to be encoded by the mouse genome, has afforded the opportunity to investigate not only the roles of these novel phosphate responsive proteins in the process of osteoblast differentiation and mineralization but also the relative roles of transcription and post-translational modifications in protein abundance.

Change in Relative Abundance after Exposure to Elevated Inorganic Phosphate—One mechanism by which proteins are regulated, and in turn regulate cell function is through changes in relative abundance. At present, it is unclear to what degree the relative abundance of a protein must be altered to result in a physiologically relevant response. It is likely that the physiologically relevant change in abundance will differ for most proteins. We have chosen to highlight proteins that have an altered abundance ratio of greater than 1.75-fold because we have previously determined that this -fold change is significantly detectable by both Northern (5) and Western (12) blotting. Table I represents a partial list of identified proteins representing multiple functional classes that are either increased or decreased by ≥1.75-fold in response to inorganic phosphate treatment for 24 h relative to control (sulfate). The number of times a peptide was identified for each protein and the average change in abundance are listed. These peptides may represent the same or unique peptides within a given protein. All proteins with increased or decreased relative abundances ≥1.75-fold are accessible in
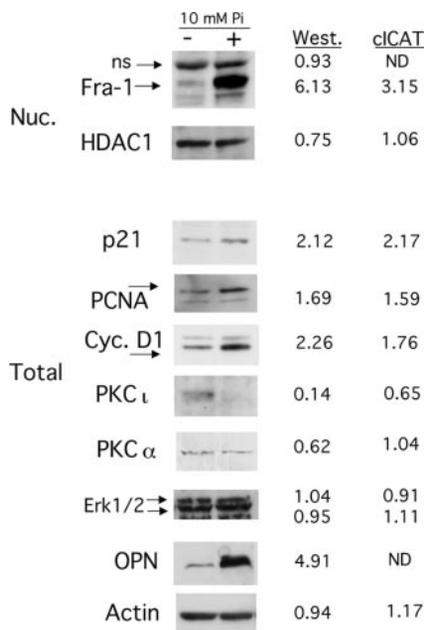
FIG. 1. **Western blot analysis of inorganic phosphate-treated MC3T3-E1 cells.** MC3T3-E1 cells were treated with either 10 mM inorganic phosphate or sulfate (control) for 24 h, and the cells were harvested for analysis. The signal intensity was quantitated, and the ratio of protein abundance, phosphate to sulfate, is listed next to the autoradiograph (*ns*, nonspecific; *ND*, no data). The corresponding abundance ratio as determined by cICAT is also listed. Note: the cyclin D1 and actin autoradiographs have been published previously (12). *Nuc.*, nuclear.

Function/Pathway analysis derived from Ingenuity pathway analysis of cICAT data of proteins with altered abundance of 1.75 or more. Protein no. represents the number of cICAT-identified proteins found in a particular functional grouping as determined by the application. Table represents functional groupings with greater than 20 protein found and significance < 1.00E-3.

Function	Significance	Protein no.
Cell cycle	1.01E-4–4.92E-2	42
DNA replication, recombination & repair	1.01E-4–4.58E-2	29
Protein synthesis	1.26E-4–4.24E-2	49
Cancer	3.12E-4–4.92E-2	44
Cell morphology	7.62E-4–4.62E-2	32
Cellular assembly and organization	7.26E-4–2.70E-2	29
Cell-to-cell signaling and interactions	8.05E-4–4.92E-2	22

abundances by densitometric analysis of the Western blot revealed a good agreement with the cICAT measured ratio in response to elevated inorganic phosphate for all conditions examined (Fig. 1) and suggests that, in fact, such global quantitative proteomic measurements can be used to accurately predict changes in relative protein abundance from complex samples in an equivalent manner to more traditional biochemical methods.

Pathway/Function Analysis of Inorganic Phosphate Regulated Proteins: Cell Cycle and Proliferation— The global scale of the cICAT labeling technique has the potential to reveal insights into entire pathways or functional relationships in response to a given stimuli. An analysis of the dataset representing all proteins with altered changes in abundance greater than 1.75, either up or down, using Ingenuity's pathway analysis application revealed a number of significant changes in functionally related processes (Table II). This analysis revealed that the expression of proteins related to cell cycle change significantly in cells exposed to inorganic phosphate. In essence, all of the highly significant functional relationships determined by the analysis represent an increase in cellular metabolism and proliferation. An interactive network of some of these proteins, generated by the pathway analysis software, is represented in Fig. 2*A*. All proteins identified in this network were up-regulated by exposure to inorganic phosphate, and the -fold increase is listed below the respective protein.

To determine whether this analysis represented a biologically relevant output, we examined the effect of inorganic phosphate on cell cycle and proliferation. MC3T3-E1 cells were treated with inorganic phosphate and harvested for analysis of cell cycle status by flow cytometry. Inorganic phosphate caused a >50% increase in the number of cells in S phase by 24 h (Fig. 2*B*). The increase in cell cycle should be accompanied by an increase in proliferation. To determine whether inorganic phosphate caused an increase in proliferation, the treated cells were analyzed by a celltiter assay as
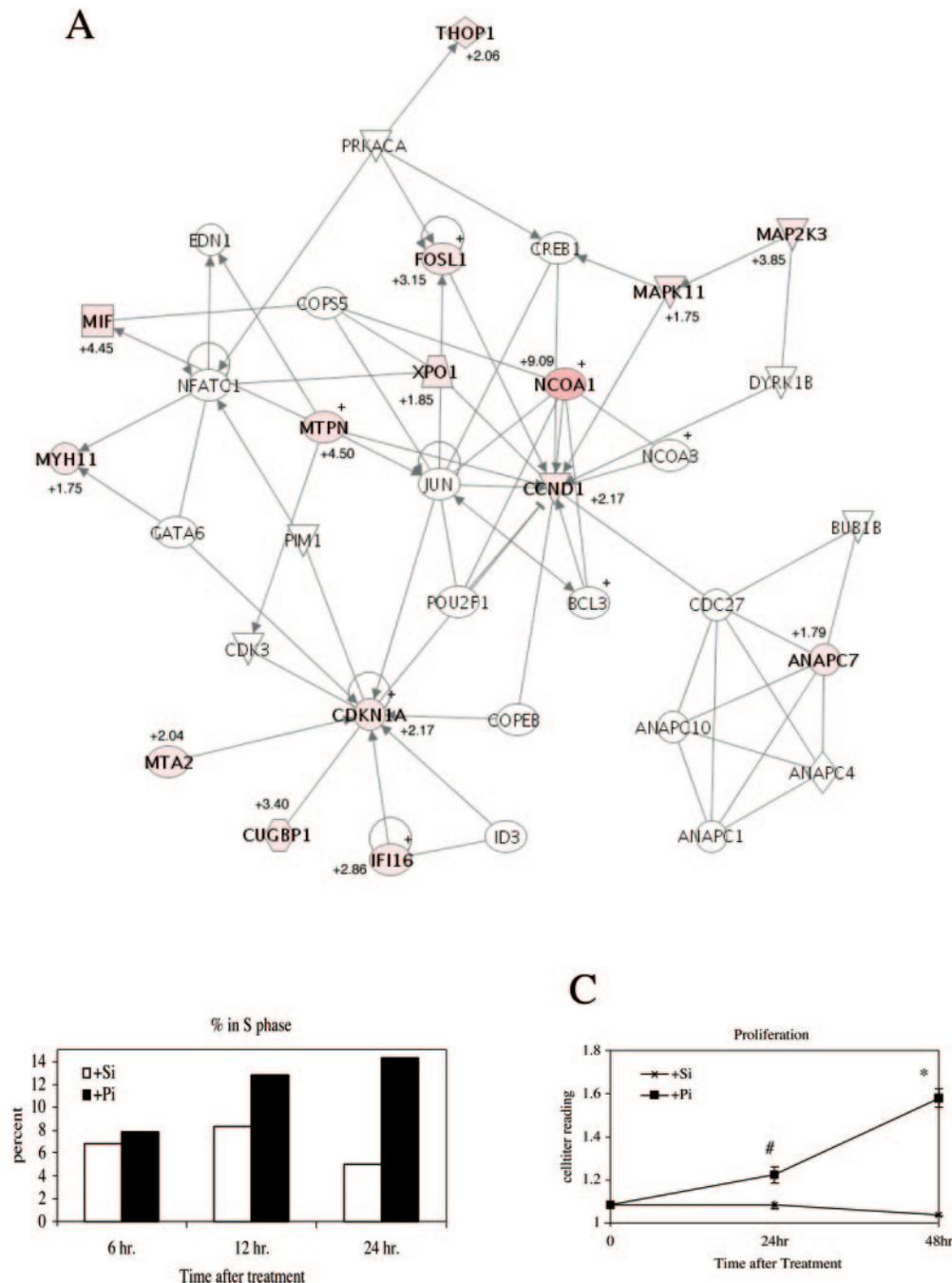
Supplemental Tables III and IV, respectively. It is clear from the results that the cICAT technique is capable of identifying classes of proteins ranging in function from extracellular matrix proteins to transcription factors, making this a powerful technique to survey protein changes on a proteome wide scale.

Validation of cICAT Quantitation by Western Blotting— Few large datasets have been generated using protein quantification techniques that will identify changes in relative protein abundance of treated samples. To determine the validity of the cICAT-derived quantitation of protein abundances described here, traditional PAGE followed by immunoblotting was performed on a series of selected proteins. Samples harvested at 24 h in parallel with the sample used for cICAT labeling were either separated into nuclear and cytoplasmic fractions or lysed as a total cell fraction and separated by polyacrylamide gel electrophoresis and electroblotted onto a membrane, which was then probed with a series of antibodies (Fig. 1). We chose to analyze proteins predicted to be either increased, decreased, or unchanged by the cICAT study, as well as proteins with different cellular locations and varying functions. In addition, we chose proteins that were identified through only a single or few peptides by cICAT (*i.e.* p21: $n = 1$) as well as proteins that were identified by a large number of peptides (*i.e.* actin: $n = 306$). Quantitation of the protein

FIG. 2. **Pathway/function analysis of phosphate regulated proteins.** *A*, cICAT-identified phosphate-regulated proteins, 1.75-fold or more (Supplemental Tables III and IV) were analyzed by Ingenuity's pathway analysis program. The analysis revealed that a number of cell cycle related proteins were increased by phosphate treatment; a network is shown here with -fold increase below each protein identified. *B*, flow cytometry was used to analyze the cell cycle status after exposure to 10 mM inorganic phosphate for times as indicated. The graph represents the percent of cells in S phase. *C*, proliferation assay of cells treated with 10 mM inorganic phosphate for indicated times. The graph represents the average of 4 individual wells and the results are representative of multiple experiments. #, $p < 0.05$; *, $p < 0.005$ (two-tailed analysis).

described under "Experimental Procedures." The celltiter results from multiple determinations (Fig. 2C) reveal an increase in proliferation starting at 24 h and extending through 48 h. The data are in good agreement with the approximate 24-h doubling time of these cells. This analysis reveals that exposure to elevated inorganic phosphate results in an increased number of cycling cells and an overall increase in proliferation. In addition, these results suggest that a global analysis of changes in relative protein abundance can in fact reveal significant and biologically relevant changes in cell function.

Comparison with Microarray Analysis—To date, because of the technical limitations of generating large proteome data-
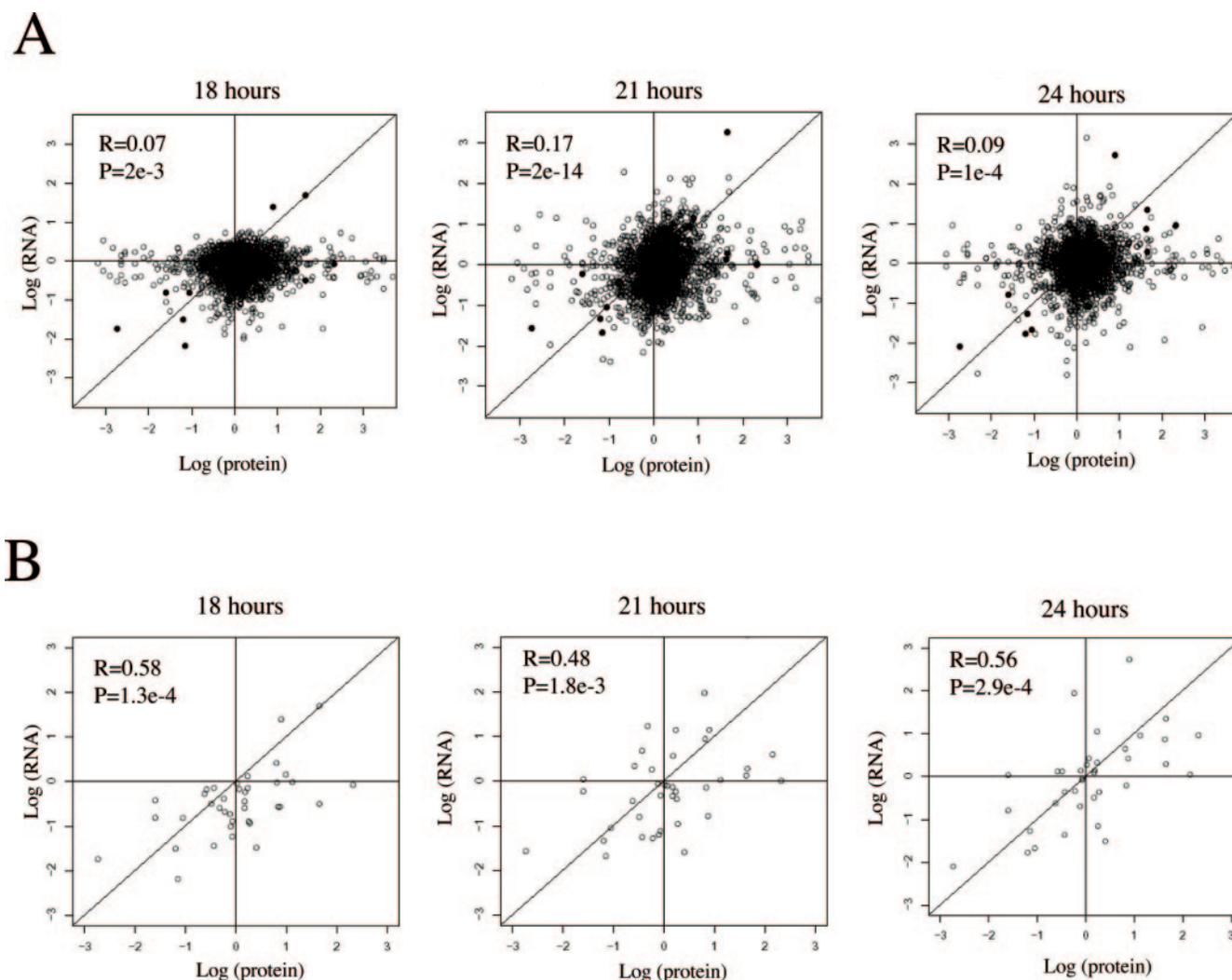
FIG. 3. **Pearson correlation of relative RNA and protein abundance at various time points after inorganic phosphate treatment.** *A*, RNA samples generated at 18, 21, and 24 h and parallel samples with cICAT (array) at 24 h after exposure to 10 mM inorganic phosphate were correlated with the relative protein abundance. *B*, osteoblast-specific genes were compared by Pearson correlation as described in *A*.

bases, there are limited data regarding the correlation of protein and mRNA levels on a global scale. The ability to conduct such correlation analyses may represent an additional and novel means to generate discrete and testable biological hypotheses from these global and discovery driven measurements. To investigate the relationship of transcription with our cICAT database, MC3T3-E1 cells were treated with 10 mM inorganic phosphate for 18, 21, and 24 h, in addition to a separate 24-hour sample harvested in parallel with the cICAT sample. The extracted mRNA samples were used to perform a NCI 22,000 oligonucleotide mRNA microarray analysis. Of the 2501 proteins identified by cICAT, ~1900 could be aligned with the corresponding genes identified in the mRNA microarray analysis, and the entire database is presented in detail in Supplemental Table V, with the 24-hour sample in parallel with cICAT listed as "array." The correlations between global mRNA levels at different time points and

corresponding protein levels at 24 h after inorganic phosphate exposure were measured by Pearson's method and are represented graphically in Fig. 3*A*. As determined by this statistical analysis, there is little correlation between RNA and protein abundance levels identified and predicted by cICAT.

To determine whether the general lack of correlation of the entire dataset also applied to tissue specific gene expression, 40 osteoblast relevant genes/proteins were chosen for correlation analysis. The genes/proteins were chosen based on previous descriptions of relevance to the osteoblast differentiation process and are listed in Supplemental Table VI. This analysis (Fig. 3*B*) revealed a much higher degree of correlation between the osteoblast specific genes/proteins than the global proteome/transcriptome correlation. The potential reasons for the general lack of correlation over the entire dataset but high correlation within the osteoblast relevant dataset are more fully explored under "Discussion."

TABLE III
Partial list of highly correlated protein/ RNA by function or pathway
No. of cases, number of cases with p value ≤ 0.05 and positive correlation from 1000 permutation; Smallest ≤ 0.05, smallest positive correlation with p value ≤ 0.05.

	Original Cor/p value(vsICAT)	Time point of correlation	No. of cases	Smallest ≤ 0.05	p Value
BioCarta Pathway					
Cell Cycle, G1-S Check Point ($n = 6$)	0.926642/0.007875	24 h	19	0.816	0.048
Cyclins and Cell Cycle Regulation ($n = 4$)	0.9679508/0.03205	24 h	32	0.951	0.049
Influence of Ras/Rho on G1 to S ($n = 10$)	0.6871/0.02816	24 h	27	0.639	0.047
Influence of Ras/Rho on G1 to S ($n = 7$)	0.7885/0.03511	Array	26	0.757	0.049
uCalpain and friends in Cell spread ($n = 10$)	0.7009515/0.02393	18 h	28	0.636	0.048
uCalpain and friends in Cell spread ($n = 10$)	0.710019/0.02142	21 h	25	0.635	0.048
uCalpain and friends in Cell spread ($n = 8$)	0.8931876/0.002808	24 h	23	0.715	0.046
GO-Term					
Cell Cycle ($n = 22$)	0.5011/0.01751	21 h	36	0.429	0.047
Integrin-mediated signaling ($n = 15$)	0.8295/0.04115	Array	20	0.816	0.048
G-protein coupled receptor signaling ($n = 15$)	0.7639/0.0009158	Array	25	0.950	0.050
Induction of Apoptosis ($n = 4$)	0.9636/0.03637	Array	25	0.950	0.050
Mitosis ($n = 7$)	0.82567/0.02214	21 h	26	0.755	0.050
Rho protein signal transduction ($n = 7$)	0.8316/0.02036	21 h	26	0.755	0.050
Rho protein signal transduction ($n = 7$)	0.82235/0.02316	21 h	26	0.755	0.050

Analysis of BioCarta Pathways and GO-Term Associated Groups Reveals a Higher Correlation between Protein and mRNA Levels within Functional Subsets—The general lack of overall correlation prompted us to examine whether subsets of genes/proteins based on function/pathway (Gene Ontology "GO" or BioCarta databases) would show higher correlations. As described under "Experimental Procedures," this analysis uses an unbiased means to determine correlation based on previously defined gene groupings. The output, a partial list of which is detailed in Table III, represents a strong correlation between protein and mRNA levels within certain pathways or functional groupings as evidenced by detection of least four genes/proteins that when correlated have a p value of less than 0.05 at any time point analyzed. The full analysis is found in Supplemental Table VII. In addition, we evaluated the likelihood that these correlations were statistically significant by permutation analysis. The analysis (Table III) revealed that for all pathway/functional groupings that demonstrated a significant correlation in the change in mRNA and protein abundance in osteoblasts exposed to inorganic phosphate, the permutation analysis showed less than 5% of permutations with significant correlations compatible with the original correlations and therefore strengthens and validates the conclusion that these groupings are significantly correlated. The identification of high correlation between protein and mRNA in the cell cycle category of both GO and Biocarta databases reflects a previously defined method of regulation, which was revealed as a regulation mechanism in many basic biological processes in many lower organisms. The correlation of certain pathway/function groupings, such as the "ucalpain and friends" subset at multiple time points also suggests that this type of analysis is a valid method for identifying pathways or functional groupings regulated through transcription/transla-

tion. These data suggest that although there is within the total proteome and transcriptome at any given time point a general lack of correlation, functional subsets of genes/proteins may still be tightly coordinately regulated. Likewise, other subsets are not coordinately regulated and may represent pathways regulated by post-translational modification.

Subtraction of Proteome and Transcriptome Databases Reveals Post-translationally Regulated Proteins: Fra-1—The ability to compare large datasets of protein and mRNA levels represents an opportunity to extract biologically meaningful data not previously possible. A comparison of the protein and mRNA data generated in this analysis revealed a number of proteins whose relative abundance was substantially increased in osteoblasts after exposure to elevated inorganic phosphate, whereas the corresponding mRNA levels show little change. Table IV reveals proteins detected with changes in abundance greater than 3.0-fold, whereas the corresponding RNA, detected by microarray, was not altered by more than 1.5-fold at any time point investigated. These proteins represent potential targets of post-translational regulation by elevated inorganic phosphate.

To experimentally validate this notion, we chose to analyze in more depth Fra-1 (*fosl1*). Fra-1 is of particular interest in that it is a member of the activator protein (AP)-1 family of transcription factors, which is important in both bone development and the regulation of osteoblast function (reviewed in Ref. 16). A Northern blot analysis of samples used for the cICAT microarray revealed no detectable changes in Fra-1 RNA (data not shown) in agreement with microarray results (Supplemental Table V). To test the hypothesis that the increase in Fra-1 protein is the result of post-translational regulation in response to elevated inorganic phosphate, we treated the pre-osteoblasts with either the translation inhibitor cycloheximide or the transcription inhibitor actinomycin D

TABLE IV
Elevated protein without corresponding RNA

Proteins identified with cICAT values >3.0 and microarray values <1.5 on all three microarrays (18, 21, and 24 hours).

Protein description	ICAT	18	21	24	Unigene
II iodothy. deiodin.	25.0		0.63		Mm.21389
AMBP protein (bikinun)	20.0	1.22			Mm.2197
7-dehydro. red.	12.9	0.76	0.55	0.95	Mm.249342
1500004O14Rik protein	11.1	1.06	1.16	0.88	Mm.306482
4930443G12Rik protein	11.1	1.01			Mm.307948
Na-dep. dopamine trans.	11.1	0.61	1.04		Mm.41993
Nucleophosmin (NPM)	10.4	1.04	1.33	1.03	Mm.6343
Steroid coactivator-1	9.09	0.84	0.68	0.84	Mm.301039
Collagen a1 XIX chain	9.09	0.74	1.34		Mm.329196
Cyto. b-5 red. (NADH)	8.54	0.69	0.81	0.94	Mm.22560
5′-3′ exoribo. 2 (Dhm1)	8.27	0.79	1.01	1.27	Mm.3065
P52rIPK	7.69	0.78	1.30	0.33	Mm.4428
0610006A11Rik protein	6.67	1.05			Mm.2202
1500016H10Rik protein	5.76	1.05	1.26	0.79	Mm.218533
PRP31	5.56	1.13	1.41	1.04	Mm.246863
Polycystin 2	5.00	1.07	0.56	1.16	Mm.6442
Ubiq.-cyto. C reduct.	4.98	0.74	1.03	1.04	Mm.334206
Thymidine kinase	4.86	1.06	1.13	0.96	Mm.2661
3110031G15Rik protein	4.76	1.18	0.59	1.14	Mm.208618
Sim. to cylindromatosis	4.76	0.93	0.62	0.80	Mm.24282
XII secr. Phopholip. A2	4.66	1.29	1.22	0.91	Mm.151951
Myotrophin (V-1)	4.60	0.75	0.61	0.89	Mm.182746
Chromobox pro. hom. 5	4.55	1.01	1.06	0.96	Mm.262059
Sim. to SUMO-1 prot. 2	4.55	0.93	0.83	0.88	Mm.255784
NADH-ubi. oxi. PDSW	4.36	0.93	1.23	1.29	Mm.1129
5730455C01Rik protein	4.35	0.80	0.66	0.87	Mm.22379
4921529O18Rik protein	4.17	0.55		0.88	Mm.266280
Pentaxin-related protein	4.17	0.30	0.38	0.26	Mm.276776
Histone H3 (H3.2)	3.52	0.75	0.49	1.24	Mm.261670
Nucleoporin-lp-1 iso..T	3.45	0.71	0.95	0.67	Mm.45513
CUG repeat RNA-bp 1	3.40	0.95	0.99	1.00	Mm.29495
Serum albumin	3.24	0.94		0.73	Mm.16773
L-lactate dehydrog. A	3.20	0.95	1.18	1.32	Mm.29324
FRA-1	3.15	0.71	1.22	1.23	Mm.6215
70 kDa WD-repeat	3.03	1.18	0.83		Mm.325512

followed by treatment with 10 mM inorganic phosphate for 24 h. The results (Fig. 4*A*) revealed an increase in Fra-1 protein in the presence of either the translation or transcription inhibitor and suggest that in fact Fra-1 is post-translationally regulated in response to inorganic phosphate. Analysis of samples harvested in parallel for mRNA levels revealed that Fra-1 is not highly regulated by transcription at this time point (Fig. 4*C*). Quantification of the Northern blot revealed an approximate 1.2-fold increase in response to phosphate (data not shown) in good agreement with the 1.23-fold increase determined in the mRNA microarray analysis (Table III). Immunoblotting for osteopontin, a positive control, revealed a strong upregulation of both protein and RNA that is completely blocked by treatment with either inhibitor. This result also demonstrated that both the cycloheximide and actinomycin D were given at a functionally relevant concentration (Fig. 4, *B* and *C*).

In addition, we sought to determine whether another known stimulator of Fra-1 protein functioned in this manner.

MC3T3-E1 cells were treated as above, but the phorbol-ester TPA was used as an inducer. The results revealed a somewhat different mode of regulation relative to inorganic phosphate (Fig. 4, *A–C*). The translation and transcription inhibitors both caused a more pronounced inhibition of TPA-induced Fra-1 levels and suggested that transcription plays a more significant role in the regulation of Fra-1 in response to TPA than inorganic phosphate at the time points analyzed. This is also evident in the larger increase in Fra-1 RNA in response to TPA than inorganic phosphate (Fig. 4*C*). Taken together, these results not only provide evidence that Fra-1 is post-translationally regulated by inorganic phosphate but also serve as a proof of principle that post-translationally regulated proteins can successfully be identified by a systems level analysis such as presented herein. Furthermore, these experiments identify inorganic phosphate as a potential key regulator of an important transcription factor, Fra-1, during osteoblast development.
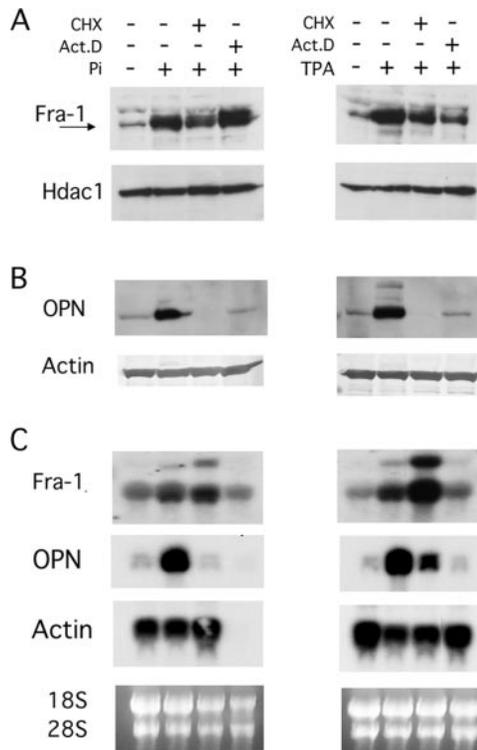
Fig. 4. **Western and Northern analysis of the post-translational regulation of Fra-1.** MC3T3-E1 cells were treated with methanol (vehicle-control), cycloheximide (1 μm), or actinomycin D (100 ng/ml) followed by addition of either 10 mM inorganic phosphate for 24 h or TPA (10 ng/ml) for 6 h. The resulting samples were fractionated, and the nuclear (*A*) and cellular (*B*) lysates were separated on a 4–12% gel. After transfer, the membranes were immunoblotted as indicated. A parallel set of samples was harvested for Northern analysis (*C*). The resulting blot was probed as indicated.

DISCUSSION

The spatial and temporal coordination of osteoblast differentiation and mineralization is a complex process requiring exquisite communication between the cell and the extracellular environment. We have described previously the significance of inorganic phosphate that is generated during osteoblast differentiation as a key signaling molecule in the process of regulated gene expression leading to mineralization (reviewed in Ref. 17). In an attempt to understand the effect of this signaling molecule on cell function at a systems level, we conducted both quantitative proteomic and gene expression analyses of inorganic phosphate-treated osteoblasts with the goal of conducting a global analysis of the relationship between regulation of the osteoblast transcriptome and the proteome in response to inorganic phosphate exposure.

Analysis of the cICAT data alone has revealed insights into the mechanism by which inorganic phosphate influences osteoblast function. A number of proteins involved in the oxidative phosphorylation pathway were strongly increased, suggesting a possible important role of mitochondria in the phosphate response. In fact, a recent study has defined inor-

ganic phosphate as a regulator of oxidative phosphorylation (18). Furthermore, a number of studies have identified the requirement of mitochondrial function and increased ATP in osteoblast mineralization and differentiation (19–21). These results in combination with the data presented here suggest that inorganic phosphate may be an important regulator of metabolic function during osteoblast differentiation. It is interesting that the results identify a general decrease in many proteins involved in β-oxidation, suggesting the ability of elevated inorganic phosphate to preferentially regulate particular metabolic pathways. The increase in metabolism agrees with our data revealing for the first time that inorganic phosphate causes an increase in the number of cells actively cycling and overall proliferation. Although more work is required to determine the significance of phosphate induced proliferation in osteoblast differentiation, this line of inquiry may also prove relevant to other cell types as suggested by an increase in thymidine incorporation in parathyroid cells exposed to elevated inorganic phosphate (6).

A complete understanding of how osteoblasts generate a mineralized matrix will undoubtedly prove useful in developing interventions to disorders of bone metabolism. This study has identified a number of proteins responsive to inorganic phosphate and previously demonstrated relevant to osteoblast function including periostin (osf-2), α2-HS glycoprotein, bF-GFR2, decorin, osteoglycin (mimecan precursor), TIMP-1, and Fra-1, among others. In fact, we have previously identified periostin, decorin, tropomyosin 2, and cyclin D1 as phosphate-responsive genes after 72 h of phosphate treatment (5). The regulation of a large number of extracellular matrix proteins suggests that inorganic phosphate may be an important signal for the transition of the matrix to a mineralization competent state. The quantitative proteomic analysis has also identified a number of proteins regulated by inorganic phosphate that were not previously known to be associated with osteoblast function including α-1 and α-2 microglobulin, AD-AMTS-2, polycystin 2, Chondroitin 4 sulfotransferase, calgizzarin, copine I, and DAAM2, among others. The response of these proteins to inorganic phosphate suggests that they may play important roles in the mid to late phases of osteoblast differentiation when inorganic phosphate levels are higher. The increased abundance of a number of proteins involved in calcium regulation agrees with previous results suggesting that as inorganic phosphate levels rise, the cell must balance the calcium-to-phosphate ratio or risk apoptosis (22).

Although much useful information can be gleaned from proteomic data alone, the ability to combine the gene expression data with corresponding protein levels on a large scale represents a novel mechanism for extracting biologically relevant results. Because the temporal relationship between transcription and translation on a large scale is not well defined, we chose to not only analyze RNA samples corresponding to the 24-h time point used for the quantitative proteomic analysis but also two time points preceding this, 18 and 21 h.

This analysis resulted in a generally low level of correlation. The lack of correlation between quantitated protein and RNA levels has been reported previously in a number of models although with smaller datasets (23–30). There may be multiple reasons for the lack of overall correlation. First, there is an inherent variability within all scientific assays and biological systems, especially in high throughput technologies such as those used in the present studies; therefore, a pure statistical comparison may not be most representative. In addition, the higher correlation between the 21-hour-treated RNA sample with the 24-h protein sample suggests that analyzing a single static time point in a dynamic system such as a cellular response to a stimulus may not be optimal. Because the temporal relationship between transcription and translation is likely to vary based on the individual gene/protein, it may not be realistic to expect a high degree of correlation between RNA and protein levels when attempting to correlate dynamic changes in RNA with a static picture of the proteome. Finally, the results described here represent a time point 24 h after stimulation, and it is possible that the longer the time from stimulation, the less likely it is that RNA and protein levels will correlate. Experiments are currently underway to address this possibility.

Although overall there was a generally low correlation, a stronger correlation was observed between several of the known osteoblast associated proteins and their corresponding RNA levels, such as periostin, osteoglycin, and TIMP-1, among others. Other studies have found some degree of correlation when looking at particular subsets of proteins (31–33). We also investigated the possibility that selected pathways and/or Gene Ontology groups may have higher or lower relative correlations. Indeed, the analysis revealed a number of subsets of proteins/RNAs that demonstrated a high degree of correlation that were subsequently validated by permutation analysis. Furthermore, the observation that the correlation of certain pathway/function groupings, such as the "ucalpain and friends" biocarta pathway exists at multiple time points may imply that there is a time-persistent type of coordination between transcription and translation that is maintained during a biological process, which might be critical for osteoblast differentiation. The identification of a high correlation between protein and RNA in certain "critical or specific" pathways or GO-groups such as cell cycle, may reflect a previously defined method of regulation or existence of global attractors of the dynamics, which has been revealed by recent biological network study in yeast as attractors or attracting trajectory (34). This may indicate that genes for certain specific biological processes may need to be better synchronized both transcriptionally and translationally for synergistic purposes. It may also suggest that "specific" effects that are a direct response of a given stimuli to the particular cell system will correlate in a more temporal manner than "bystander" or "housekeeping" effects that are activated to maintain cell homeostasis. Information surrounding the degree of correlation between transcription and translation within certain functional groupings or pathways may prove useful in designing strategies for therapeutic intervention.

Although many of the osteoblast specific genes/proteins correlated well, a few did not. Subtraction of the RNA and protein databases has revealed a number of proteins regulated without concurrent increases in RNA at any time point analyzed. One such protein, Fra-1, is a member of the AP-1 family of bzip transcription factors. Genetic manipulation of *AP-1* genes through either transgenic or knockout mice, have revealed that most AP-1 family members play important roles in osteoblast development and bone metabolism (reviewed in Ref. 35). In particular, Fra-1 has been demonstrated to be a key transcription factor in bone metabolism either by transgenic expression (36) or conditional loss of function (37). The recently reported conditional loss-of-function mice developed osteopenia characterized by progressive loss of bone mass, suggesting an important role for Fra-1 in osteoblast function. Furthermore, these authors suggest that Fra-1 is likely to function at the mid to late stages of osteoblast maturation, a time that corresponds to elevated inorganic phosphate. Transgenic expression of Fra-1 revealed a dramatic increase in postnatal bone mass of the entire skeleton, in part because of a increased number of osteoblasts (36). These studies clearly demonstrate the significance of Fra-1 in osteoblast function as it relates to bone metabolism.

Although many of the AP-1 genes/proteins have been linked to bone metabolism, little is known about the forces that regulate this family of transcription factors during bone metabolism. Data presented here identify post-translational modification as a regulator of Fra-1 in osteoblasts. Previous studies suggest a mechanism by which Fra-1 is post-translationally regulated. The phosphorylation of Fra-1 by the mitogen-activated protein kinases ERK1/2 has been demonstrated to protect Fra-1 from proteosomal degradation (38) and to result in post-translational stabilization (39). We have previously demonstrated that ERK1/2 is activated by elevated inorganic phosphate at 24 h (4), which suggests a possible mechanism by which Fra-1 is post-translationally regulated in this model. The identification of inorganic phosphate as a regulator of Fra-1 during osteoblast differentiation represents a novel mechanism by which the activity of the translational but not transcriptional machinery is coordinated with the extracellular environment, and represents one of the first identifications of a regulator of the AP-1 family of transcription factors in bone metabolism.

In conclusion, the studies presented here describe the successful combination of large scale proteomic and microarray datasets to determine at least three novel mechanisms by which inorganic phosphate regulates cell function (Fig. 5). 1) Analysis of the cICAT data defined novel phosphate responsive proteins and revealed the regulation of pathways or functional networks involved in cell cycle, proliferation and energy metabolism. 2) A comparison of the cICAT-derived protein
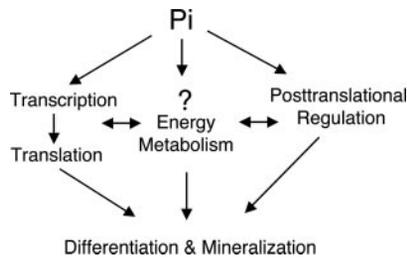
FIG. 5. **Mechanisms of inorganic phosphate affect on cell function.** The combined proteomic and microarray studies presented here suggest at least three novel mechanisms by which inorganic phosphate affects cell function: an increase in cellular energy metabolism, increased transcription/translation, and targeted post-translational stability. The significance is 2-fold: 1) the ability to identify these regulatory mechanisms was made possible only by combining these global analyses and emphasizes the power of such an approach, and 2) data generated from this approach have identified biologically relevant consequences of elevated inorganic phosphate in the process of differentiation and mineralization.

data with microarray samples has led to the determination that osteoblast-specific genes are more likely to be tightly regulated by the traditional transcription/translation pathways. 3) Furthermore, this type of comparison can led to novel methods of data extraction, including the identification of post-translationally regulated proteins as evidenced by Fra-1. A future challenge will be to determine how these signals are integrated in a complex process that spans weeks and months. The data presented here not only reveal novel insights into the role of inorganic phosphate in altering cell function but also provide an initial glimpse at the power of combining large scale protein and mRNA analysis for a systems level understanding of the cell.

Ⓢ The on-line version of this article (available at http://www.mcponline.org) contains Supplemental Tables I–VII.

§ These authors contributed equally to this work.

** To whom correspondence should be addressed. Tel.: 301-846-1651; Fax: 301-846-6907; E-mail: gbeck@ncifcrf.gov.

REFERENCES

1. Quarles, L. D., Yohay, D. A., Lever, L. W., Caton, R., and Wenstrup, R. J. (1992) Distinct proliferative and differentiated stages of murine MC3T3-E1 cells in culture: an *in vitro* model of osteoblast development. *J. Bone Miner. Res.* **7,** 683–692
2. Sudo, H., Kodama, H. A., Amagai, Y., Yamamoto, S., and Kasai, S. (1983) *In vitro* differentiation and calcification in a new clonal osteogenic cell line derived from newborn mouse calvaria. *J. Cell Biol.* **96,** 191–198
3. Franceschi, R. T., and Iyer, B. S. (1992) Relationship between collagen synthesis and expression of the osteoblast phenotype in MC3T3-E1 cells. *J. Bone Miner. Res.* **7,** 235–246
4. Beck, G. R., Jr., and Knecht, N. (2003) Osteopontin regulation by inorganic phosphate is ERK1/2-, protein kinase C-, and proteasome-dependent. *J. Biol. Chem.* **278,** 41921–41929
5. Beck, G. R., Jr., Moran, E., and Knecht, N. (2003) Inorganic phosphate regulates multiple genes during osteoblast differentiation, including Nrf2. *Exp. Cell Res.* **288,** 288–300
6. Roussanne, M. C., Lieberherr, M., Souberbielle, J. C., Sarfati, E., Drueke, T., and Bourdeau, A. (2001) Human parathyroid cell proliferation in response to calcium, NPS R-467, calcitriol and phosphate. *Eur. J. Clin. Investig.* **31,** 610–616
7. Glinn, M., Ni, B., Irwin, R. P., Kelley, S. W., Lin, S. Z., and Paul, S. M. (1998) Inorganic Pi increases neuronal survival in the acute early phase following excitotoxic/oxidative insults. *J. Neurochem.* **70,** 1850–1858
8. Kido, S., Miyamoto, K., Mizobuchi, H., Taketani, Y., Ohkido, I., Ogawa, N., Kaneko, Y., Harashima, S., and Takeda, E. (1999) Identification of regulatory sequences and binding proteins in the type II sodium/phosphate cotransporter NPT2 gene responsive to dietary phosphate. *J. Biol. Chem.* **274,** 28256–28263
9. Jono, S., McKee, M. D., Murry, C. E., Shioi, A., Nishizawa, Y., Mori, K., Morii, H., and Giachelli, C. M. (2000) Phosphate regulation of vascular smooth muscle cell calcification. *Circ. Res.* **87,** E10–E17
10. Mansfield, K., Teixeira, C. C., Adams, C. S., and Shapiro, I. M. (2001) Phosphate ions mediate chondrocyte apoptosis through a plasma membrane transporter mechanism. *Bone* **28,** 1–8
11. Takeyama, S., Yoshimura, Y., Deyama, Y., Sugawara, Y., Fukuda, H., and Matsumoto, A. (2001) Phosphate decreases osteoclastogenesis in coculture of osteoblast and bone marrow. *Biochem. Biophys. Res. Commun.* **282,** 798–802
12. Conrads, K. A., Yu, L. R., Lucas, D. A., Zhou, M., Chan, K. C., Simpson, K. A., Schaefer, C. F., Issaq, H. J., Veenstra, T. D., Beck, G. R., Jr., and Conrads, T. P. (2004) Quantitative proteomic analysis of inorganic phosphate-induced murine MC3T3-E1 osteoblast cells. *Electrophoresis* **25,** 1342–1352
13. Young, M. R., Nair, R., Bucheimer, N., Tulsian, P., Brown, N., Chapp, C., Hsu, T. C., and Colburn, N. H. (2002) Transactivation of Fra-1 and consequent activation of AP-1 occur extracellular signal-regulated kinase dependently. *Mol. Cell. Biol.* **22,** 587–598
14. Fisher, L. W., Stubbs, J. T., III, and Young, M. F. (1995) Antisera and cDNA probes to human and certain animal model bone matrix noncollagenous proteins. *Acta Orthop. Scand. Suppl.* **266,** 61–65
15. Beck, G. R., Jr., Sullivan, E. C., Moran, E., and Zerler, B. (1998) Relationship between alkaline phosphatase levels, osteopontin expression, and mineralization in differentiating MC3T3-E1 osteoblasts. *J. Cell. Biochem.* **68,** 269–280
16. Wagner, E. F. (2002) Functions of AP1 (Fos/Jun) in bone development. *Ann. Rheum. Dis.* **61** (Suppl. 2), ii40–ii42
17. Beck, G. R., Jr. (2003) Inorganic phosphate as a signaling molecule in osteoblast differentiation. *J. Cell. Biochem.* **90,** 234–243
18. Bose, S., French, S., Evans, F. J., Joubert, F., and Balaban, R. S. (2003) Metabolic network control of oxidative phosphorylation: multiple roles of inorganic phosphate. *J. Biol. Chem.* **278,** 39155–39165
19. Klein, B. Y., Gal, I., Libergal, M., and Ben-Bassat, H. (1996) Opposing effects on mitochondrial membrane potential by malonate and levamisole, whose effect on cell-mediated mineralization is antagonistic. *J. Cell. Biochem.* **60,** 139–147
20. Komarova, S. V., Ataullakhanov, F. I., and Globus, R. K. (2000) Bioenergetics and mitochondrial transmembrane potential during differentiation of cultured osteoblasts. *Am. J. Physiol.* **279,** C1220–C1229
21. Johnson, K., Jung, A., Murphy, A., Andreyev, A., Dykens, J., and Terkeltaub, R. (2000) Mitochondrial oxidative phosphorylation is a downstream regulator of nitric oxide effects on chondrocyte matrix synthesis and mineralization. *Arthritis Rheum.* **43,** 1560–1570
22. Adams, C. S., Mansfield, K., Perlot, R. L., and Shapiro, I. M. (2001) Matrix regulation of skeletal cell apoptosis. Role of calcium and phosphate ions. *J. Biol. Chem.* **276,** 20316–20322
23. Ideker, T., Thorsson, V., Ranish, J. A., Christmas, R., Buhler, J., Eng, J. K., Bumgarner, R., Goodlett, D. R., Aebersold, R., and Hood, L. (2001) Integrated genomic and proteomic analyses of a systematically perturbed metabolic network. *Science* **292,** 929–934
24. Heijne, W. H., Stierum, R. H., Slijper, M., van Bladeren, P. J., and van Ommen, B. (2003) Toxicogenomics of bromobenzene hepatotoxicity: a

combined transcriptomics and proteomics approach. *Biochem. Pharmacol.* **65,** 857–875

25. Gygi, S. P., Rochon, Y., Franza, B. R., and Aebersold, R. (1999) Correlation between protein and mRNA abundance in yeast. *Mol. Cell. Biol.* **19,** 1720–1730

26. Fessler, M. B., Malcolm, K. C., Duncan, M. W., and Worthen, G. S. (2002) A genomic and proteomic analysis of activation of the human neutrophil by lipopolysaccharide and its mediation by p38 mitogen-activated protein kinase. *J. Biol. Chem.* **277,** 31291–31302

27. Griffin, T. J., Gygi, S. P., Ideker, T., Rist, B., Eng, J., Hood, L., and Aebersold, R. (2002) Complementary profiling of gene expression at the transcriptome and proteome levels in *Saccharomyces cerevisiae. Mol. Cell. Proteomics* **1,** 323–333

28. Greenbaum, D., Jansen, R., and Gerstein, M. (2002) Analysis of mRNA expression and protein abundance data: an approach for the comparison of the enrichment of features in the cellular population of proteins and transcripts. *Bioinformatics* **18,** 585–596

29. Chen, G., Gharib, T. G., Huang, C. C., Taylor, J. M., Misek, D. E., Kardia, S. L., Giordano, T. J., Iannettoni, M. D., Orringer, M. B., Hanash, S. M., and Beer, D. G. (2002) Discordant protein and mRNA expression in lung adenocarcinomas. *Mol. Cell. Proteomics* **1,** 304–313

30. Kim, C. H., Kim do, K., Choi, S. J., Choi, K. H., Song, K. S., Chi, J., Koo, J. S., Hwang, S. Y., Yoon, J. H., and Seong, J. K. (2003) Proteomic and transcriptomic analysis of interleukin-1beta treated lung carcinoma cell line. *Proteomics* **3,** 2454–2471

31. Washburn, M. P., Koller, A., Oshiro, G., Ulaszek, R. R., Plouffe, D., Deciu, C., Winzeler, E., and Yates, J. R., III (2003) Protein pathway and complex clustering of correlated mRNA and protein expression analyses in Saccharomyces cerevisiae. *Proc. Natl. Acad. Sci. U. S. A.* **100,** 3107–3112

32. White, S. L., Gharbi, S., Bertani, M. F., Chan, H. L., Waterfield, M. D., and Timms, J. F. (2004) Cellular responses to ErbB-2 overexpression in human mammary luminal epithelial cells: comparison of mRNA and protein expression. *Br. J. Cancer* **90,** 173–181

33. Johnson, M. D., Yu, L. R., Conrads, T. P., Kinoshita, Y., Uo, T., Matthews, J. D., Lee, S. W., Smith, R. D., Veenstra, T. D., and Morrison, R. S. (2004) Proteome analysis of DNA damage-induced neuronal death using high throughput mass spectrometry. *J. Biol. Chem.* **279,** 26685–26697

34. Li, F., Long, T., Lu, Y., Ouyang, Q., and Tang, C. (2004) The yeast cell-cycle network is robustly designed. *Proc. Natl. Acad. Sci. U. S. A.* **101,** 4781–4786

35. Karsenty, G., and Wagner, E. F. (2002) Reaching a genetic and molecular understanding of skeletal development. *Dev. Cell* **2,** 389–406

36. Jochum, W., David, J. P., Elliott, C., Wutz, A., Plenk, H., Jr., Matsuo, K., and Wagner, E. F. (2000) Increased bone formation and osteosclerosis in mice overexpressing the transcription factor Fra-1. *Nat. Med.* **6,** 980–984

37. Eferl, R., Hoebertz, A., Schilling, A. F., Rath, M., Karreth, F., Kenner, L., Amling, M., and Wagner, E. F. (2004) The Fos-related antigen Fra-1 is an activator of bone matrix formation. *EMBO J.* **23,** 2789–2799

38. Vial, E., and Marshall, C. J. (2003) Elevated ERK-MAP kinase activity protects the FOS family member FRA-1 against proteasomal degradation in colon carcinoma cells. *J. Cell Sci.* **116,** 4957–4963

39. Casalino, L., De Cesare, D., and Verde, P. (2003) Accumulation of Fra-1 in ras-transformed cells depends on both transcriptional autoregulation and MEK-dependent post-translational stabilization. *Mol. Cell. Biol.* **23,** 4401–4415